Supplementary Material

A Mitochondrial-Targetable Dual-Functional Near-Infrared Fluorescent Probe to Monitor pH and H_2O_2 in Living Cells and Mice

Xueyuan Bi [a], Yingying Wang [a], Dandan Wang [a], Liming Liu [a], Wen Zhu [a], Junjie Zhang [b], Xiaoming Zha [a, *]

[a] *School of Engineering,* [b] *School of Pharmacy, China Pharmaceutical University, 639 Longmian Avenue, Nanjing 211198, China*

*Author for correspondence.

Email address: xmzha@cpu.edu.cn (X. Z.)

Table of contents

1. The limit of detection measurement

The detection limit of **NIR-pH-H_2O_2** towards H_2O_2 was determined through fluorescence titration. The standard deviation of the blank solution was also measured for 10 times. After the linear slope of fluorescence intensity vs. concentrations of H_2O_2 was obtained, the detection of limit (LOD) was calculated by following equation:

$$LOD = 3\sigma/\kappa$$

Where σ denotes the standard deviation of blank measurement, κ denotes the slope of the fluorescence intensity vs. H_2O_2 concentrations.

2. Comparison of fluorescent probes for H_2O_2 with the similar active group

Table S1. Comparison of **NIR-pH-H_2O_2** with fluorescent H_2O_2 probes in literature.

Probes	H_2O_2 response				pH Response	Imaging application	Reference
	Stokes Shift (nm)	LOD (μM)	Response time (min)	Detection medium			
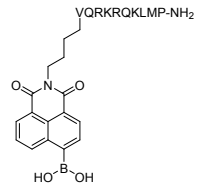	148	*	120	*	NO	HeLa cells	[1]
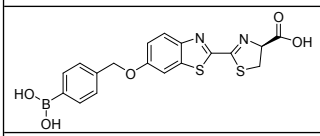	50	0.037	60	Tris buffer	NO	LNCaP-luc cells, mice	[2]
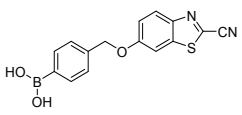	50	0.5	60	Tris buffer	NO	PC3M-luc cells, mice	[3]
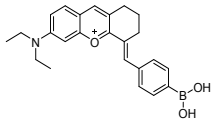	105	1.67	*	PBS buffer (1% EtOH)	NO	HeLa cells, liver tissue	[4]
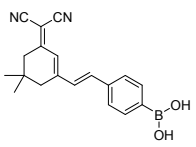	120	0.0056	35	DMSO:PBS (1:1, v/v)	NO	HeLa cells	[5]

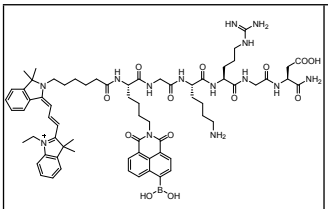	192	0.26	120	PBS buffer	NO	SKOV-3 cells	[6]
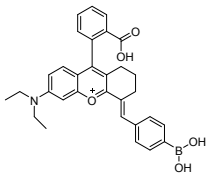	50	1.4 (pH 8) 0.99 (pH 10)	80 (pH 8), 60 (pH 10)	alkaline environment (pH > 8)	NO	Endogenous H_2O_2 in RAW 264.7 and A431 cells, mice	[7]
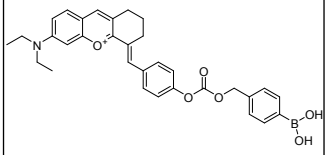	120	2.097	30 (pH 7.4)	PBS buffer (6% CH_3CN)	p*K*a = 6.17 (pH = 4 ~ 8)	Exogenous and endogenous H_2O_2 and pH in MCF-7 and Hela cells, mice	This work

* The data was not mentioned.

3. Time-dependent fluorescence changes of target probe NIR-pH-H_2O_2 for H_2O_2

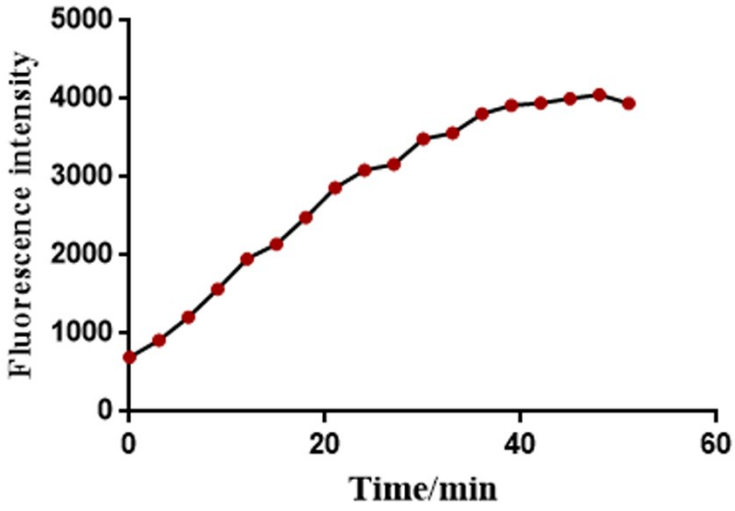

Fig. S1 Time-dependent fluorescent emission changes of **NIR-pH-H_2O_2** (10 μM) with time after addition 200 μM H_2O_2 in PBS buffer (6% CH_3CN). (λ_{ex} = 560 nm, λ_{em} = 680 nm)

4. The response between NIR-pH-H_2O_2 and H_2O_2 at different pH

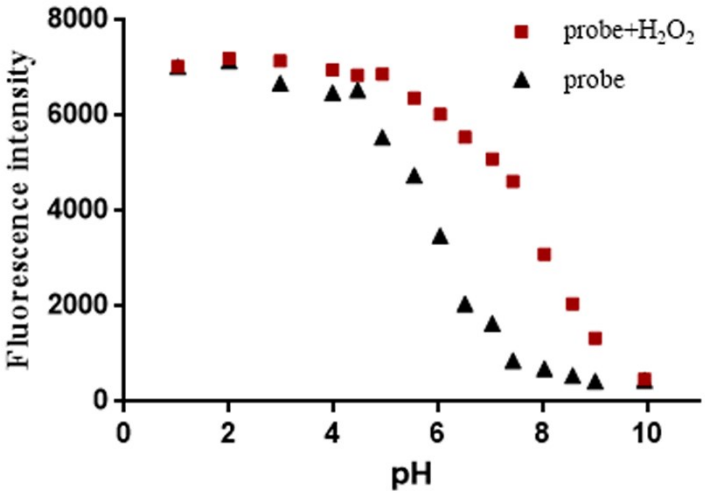

Fig. S2 Fluorescence intensity (at 680 nm) of **NIR-pH-H_2O_2** (10 μM) and **NIR-pH- H_2O_2** + H_2O_2 (200 μM) in 50 mM PBS bu□er at pH 1 to 10. (λ_{ex} = 560 nm, λ_{em} = 680 nm).

5. Fluorescent imaging in living cells

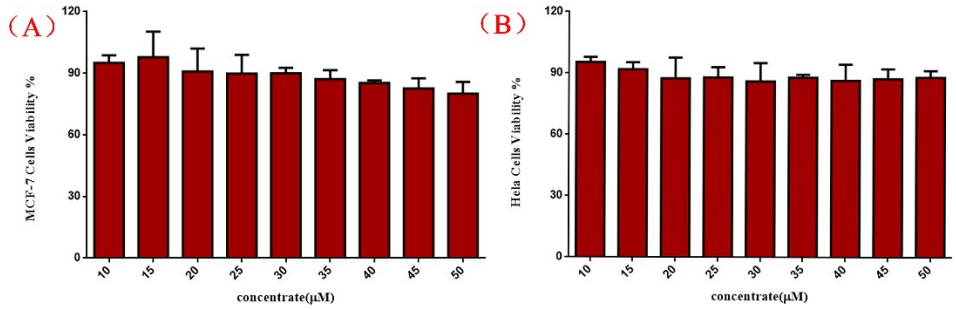

Fig. S3 MTT toxicity test for determination of cellular activity in MCF-7 cells (A) and Hela cells (B) treated with different concentrations (10, 15, 20, 25, 30, 35, 40, 45 and 50 μM) of **NIR-pH-H_2O_2** for 24 hours.

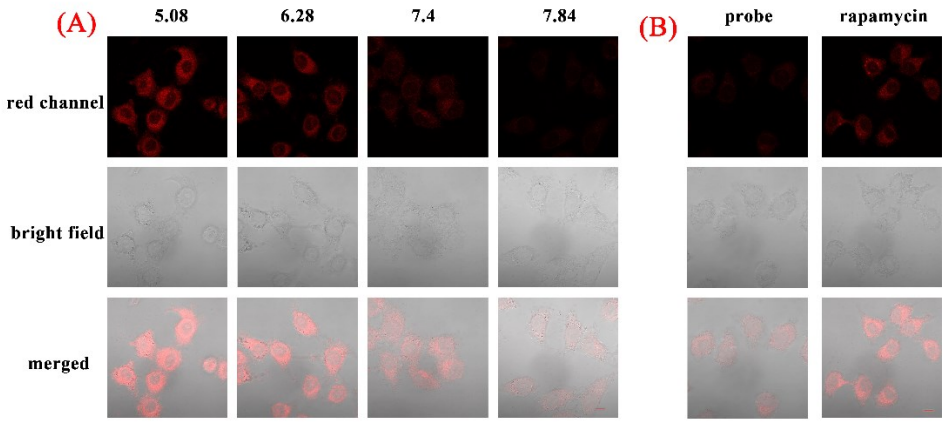

Fig. S4 Fluorescent microscopic images of Hela cells with **NIR-pH-H_2O_2** with different pH (A) and rapamycia (B). Scale bar: 10 μm.

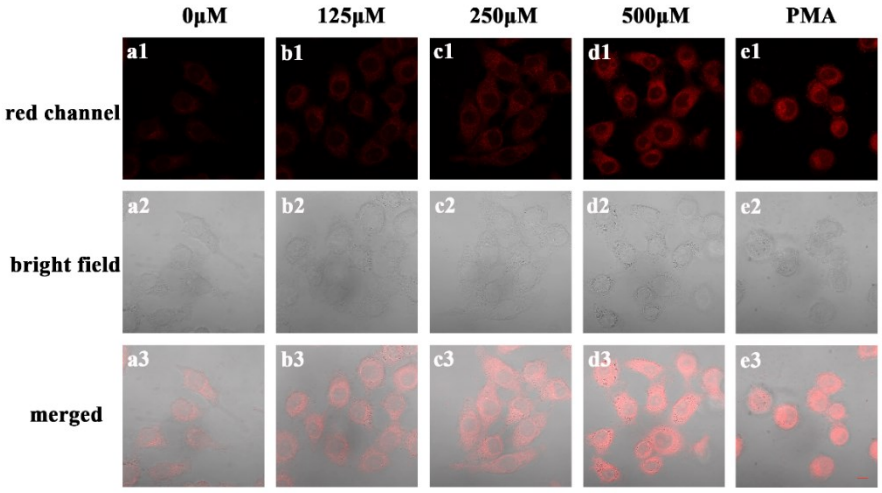

Fig. S5 Fluorescence images of **NIR-pH-H_2O_2** (10 μM) with various concentrations of H_2O_2 solution in Hela cells. Scale bar: 10 μm.

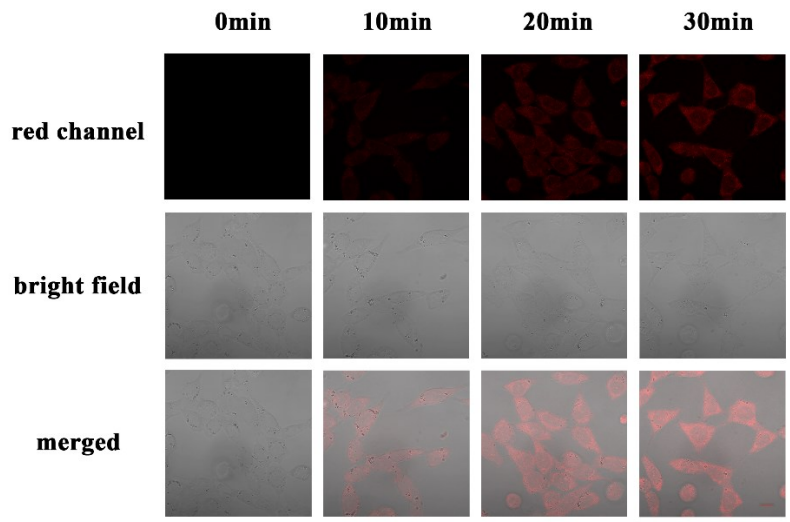

Fig. S6 Confocal fluorescence images of H_2O_2 in MCF-7 cells. Cells were pretreated with **NIR-pH-H_2O_2** (10 μM) and H_2O_2 (500 μM) for 0, 10, 20, 30 min respectively, then imaged. Scale bar: 10 μm. (λ_{ex} = 555 nm, λ_{em} = 680 nm for the red channel).

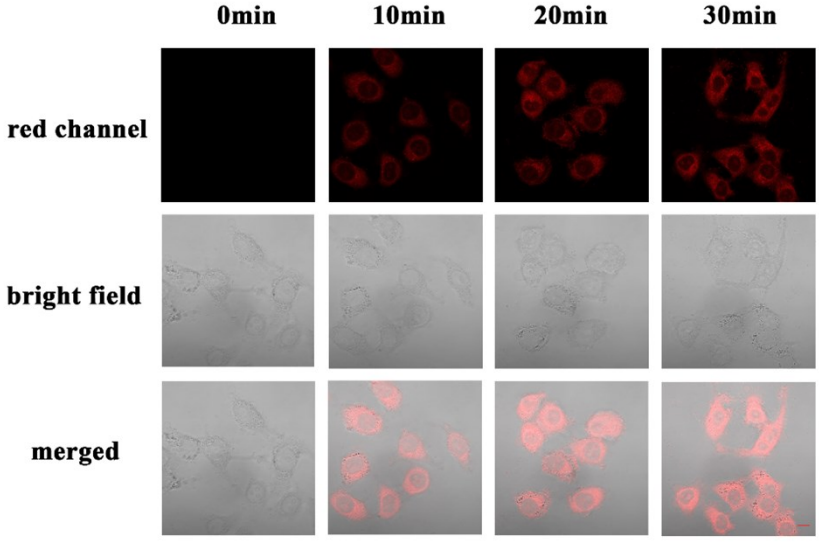

Fig. S7 Confocal fluorescence images of H_2O_2 in Hela cells. Cells were pretreated with **NIR-pH-H_2O_2** (10 μM) and H_2O_2 (500 μM) for 0, 10, 20, 30 min respectively, then imaged. Scale bar: 10 μm. (λ_{ex} = 555 nm, λ_{em} = 680 nm for the red channel).

6. ^{1}H NMR, ^{13}C NMR and MS spectrum of the probe NIR-pH-H_2O_2

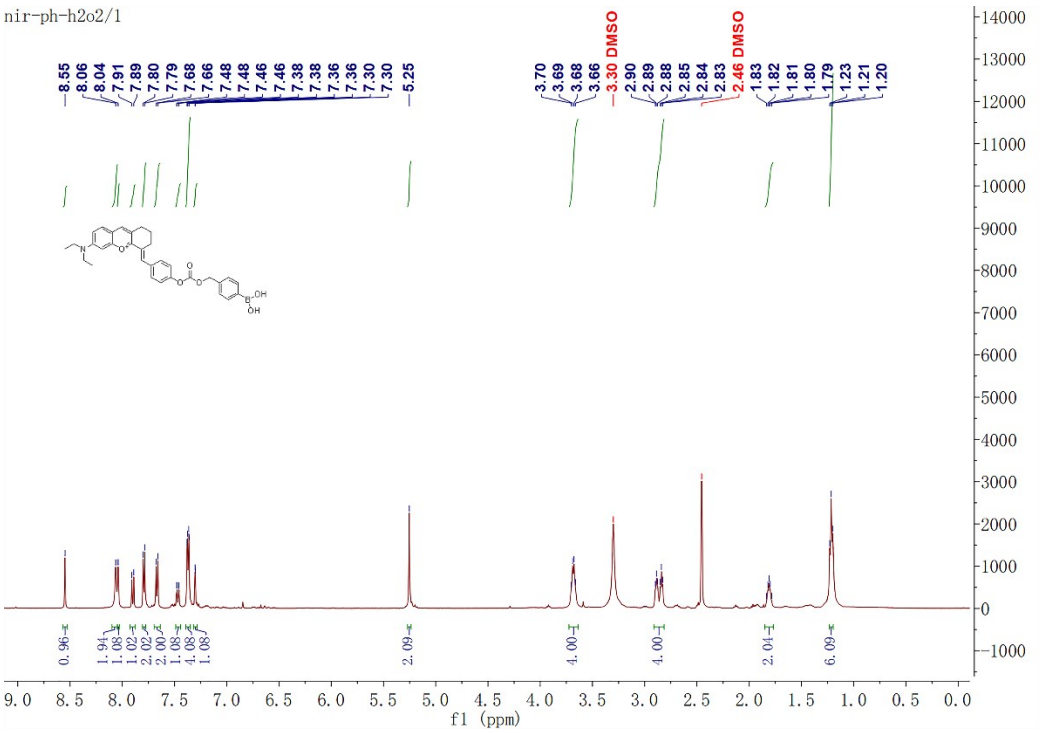

Fig. S8 ^{1}H NMR spectrum of the probe **NIR-pH-H_2O_2**.

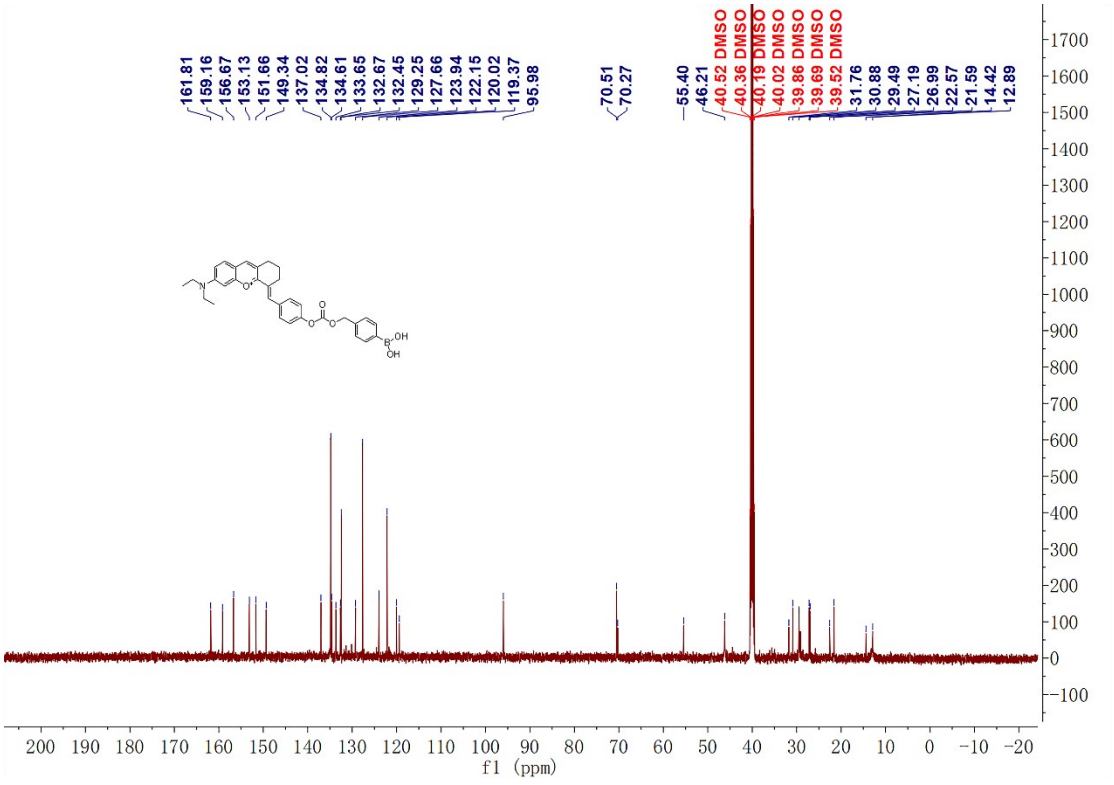

Fig. S9 ^{13}C NMR spectrum of the probe **NIR-pH-H_2O_2**

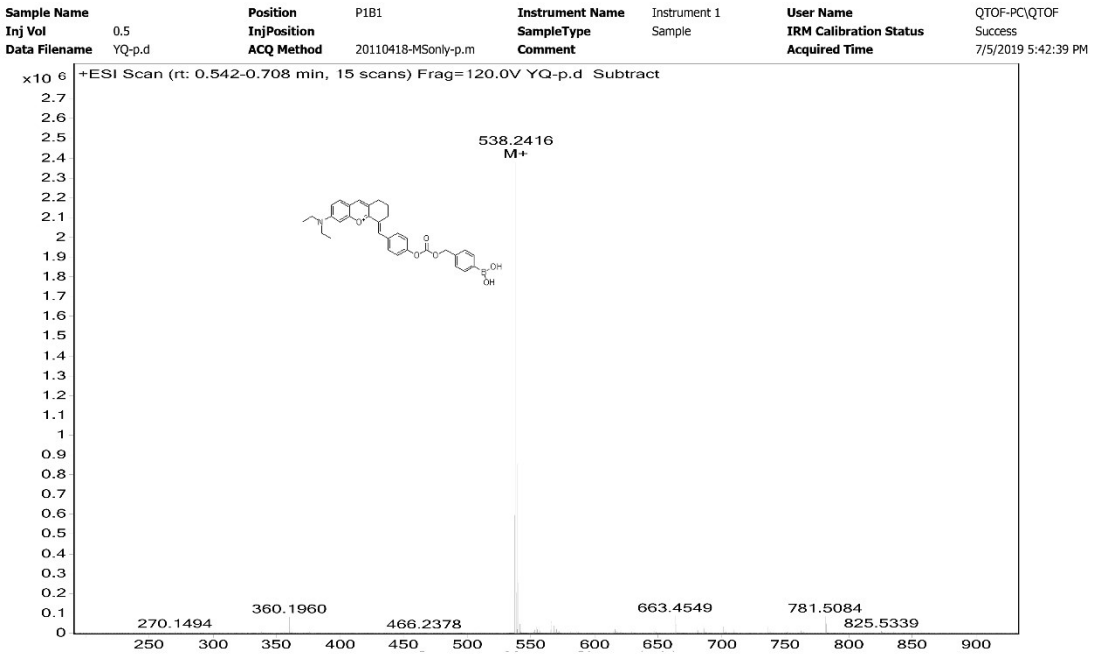

Fig. S10 HRMS spectrum of the probe **NIR-pH-H_2O_2**

7. The HPLC purity of the probe NIR-pH-H_2O_2

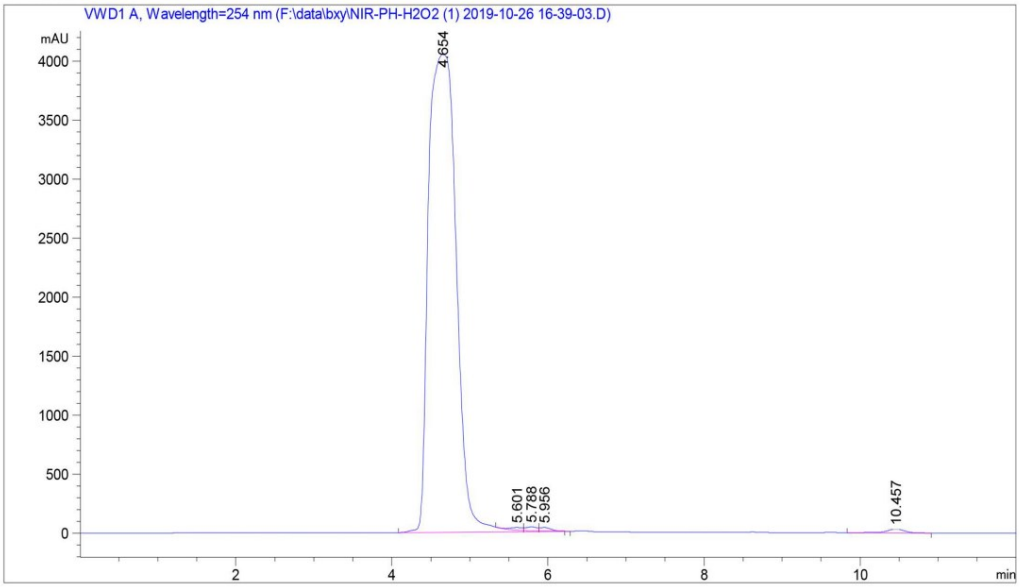

==========

面积百分比报告

==========

排序 : 信号
乘积因子 : 1.0000
稀释因子 : 1.0000
内标使用乘积因子和稀释因子

信号 1: VWD1 A, Wavelength=254 nm

峰 #	保留时间 [min]	类型	峰宽 [min]	峰面积 [mAU*s]	峰高 [mAU]	峰面积 %
1	4.654	BV R	0.3992	9.97005e4	4049.76270	98.5473
2	5.601	VV E	0.1603	249.23721	23.02718	0.2464
3	5.788	VV E	0.1483	350.59781	33.99863	0.3465
4	5.956	VB E	0.1455	301.52777	30.99067	0.2980

峰 #	保留时间 [min]	类型	峰宽 [min]	峰面积 [mAU*s]	峰高 [mAU]	峰面积 %
5	10.457	VB R	0.2347	568.38464	33.71923	0.5618

总量 : 1.01170e5 4171.49841

Fig. S11 The HPLC purity of **NIR-pH-H_2O_2**.

8. HRMS spectrum of the reaction product of the probe NIR-pH-H_2O_2 with H_2O_2

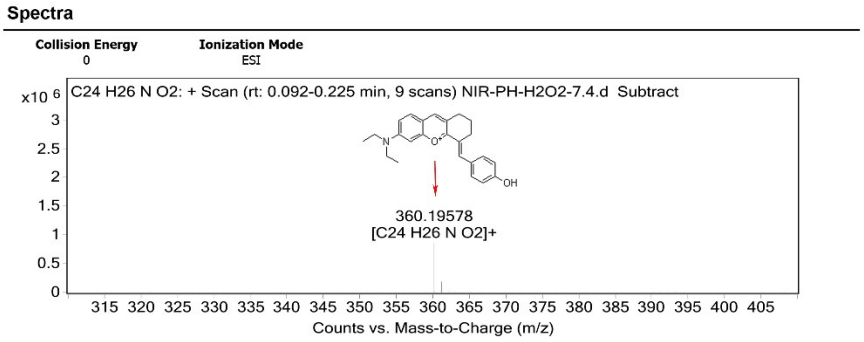

Fig. S12 HRMS spectrum of the reaction product of the probe **NIR-pH-H_2O_2** with H_2O_2.

9. HPLC analysis of the reaction product of the probe NIR-pH-H_2O_2 with H_2O_2

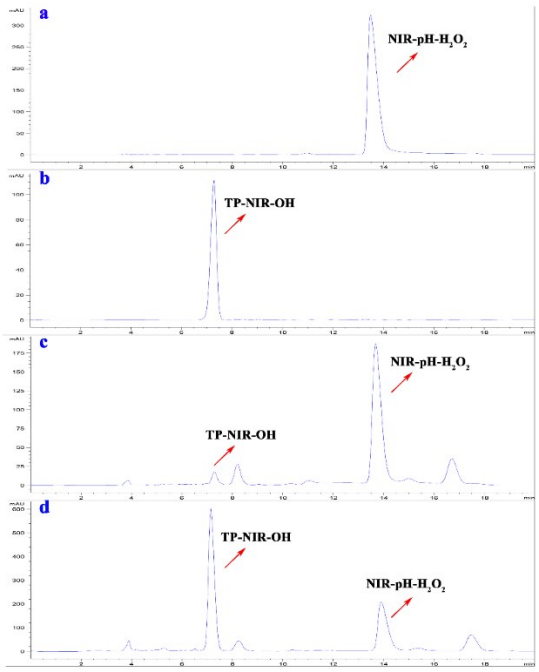

Fig. S13 HPLC changes of **NIR-pH-H_2O_2** (50 μM), **TP-NIR-OH**, **NIR-pH-H_2O_2** (50 μM) + H_2O_2 (25 μM) and **NIR-pH-H_2O_2** (50 μM) + H_2O_2 (100 μM) in PBS-Buffer (CH3CN, V/V, 6%) at pH 7.4. (A) The probe **NIR-pH-H_2O_2** (50 μM) (B) The fluorophore **TP-NIR-OH** (50 μM) (C) the probe **NIR-pH-H_2O_2** (50 μM) + H_2O_2 (25 μM). (D) The probe **NIR-pH-H_2O_2** (50 μM) + H_2O_2

(100 μM).

References

1 Y. Wen, K. Liu, H. Yang, Y. Li, H. Lan, Y. Liu, X. Zhang, T. Yi, *Anal. Chem.*, 2014, **86**, 9970–9976.

2 G.C. van de Bittner, E.A. Dubikovskaya, C.R. Bertozzi, C.J. Chang, *Proc. Natl. Acad. Sci. U. S. A.*, 2010, **107**, 21316–21321.

3 G.C. van de Bittner, C.R. Bertozzi, C.J. Chang, *J. Am. Chem. Soc.*, 2013, **135**, 1783–1795.

4 L. Zhou, H. Ding, W. Zhao, S. Hu, *Spectrochim. Acta A Mol. Biomol. Spectrosc.*, 2019, **206**, 529–534.

5 T. Wang, X. Yang, J. Men, J. Zhou, H. Zhang, *Luminescence*, 2020, **35**, 208–214.

6 P. Zhao, K. Wang, X. Zhu, Y. Zhou, J. Wu, *Dyes & Pigment.*, 2018, **155**, 143–149.

7 K. Liu, H. Shang, X. Kong, M. Ren, J.-Y. Wang, Y. Liu, W. Lin, *Biomaterials*, 2016, **100**, 162–171.